

## Fabrication of Flexible PVA/Polyaniline/WS<sub>2</sub> Composite Film and Its High Capacitance Behaviors

Aiqin Liang<sup>1,#</sup>, Danhua Zhu<sup>1,#</sup>, Liming Xu<sup>1</sup>, Weiqiang Zhou<sup>1,\*</sup>, Jingkun Xu<sup>1,\*</sup>, Xuemin Duan<sup>2</sup>

<sup>1</sup> Jiangxi Engineering Laboratory of Waterborne Coatings, Jiangxi Science and Technology Normal University, Nanchang 330013, People's Republic of China

<sup>2</sup> School of Pharmacy, Jiangxi Science and Technology Normal University, Nanchang 330013, People's Republic of China

\*E-mail: [zhouwqh@163.com](mailto:zhouwqh@163.com), [xujingkun@tsinghua.org.cn](mailto:xujingkun@tsinghua.org.cn).

Received: 26 September 2019 / Accepted: 5 July 2020 / Published: 31 August 2020

---

A flexible ternary composite film based on polyvinyl alcohol (PVA), polyaniline (PANI) and WS<sub>2</sub> was prepared *via* the electropolymerization of the prefabricated PVA/aniline/WS<sub>2</sub> hydrogel. As-prepared PVA/PANI/WS<sub>2</sub> composite film was characterized by scanning electron microscopy, X-ray photoelectron spectroscopy, energy dispersive X-ray spectrometry, and electrochemical technologies. The PVA/PANI/WS<sub>2</sub> film had a specific capacitance of 2437 mF cm<sup>-2</sup> at 2 mV s<sup>-1</sup> in H<sub>2</sub>SO<sub>4</sub> solution (1.0 M). After 5000 cycles, the capacitance retention reached 70% of initial specific capacitance. The high electrochemical behavior of composite film was mainly attributed to the ionic conductivity of PVA and the integration of pseudocapacitance of PANI and WS<sub>2</sub>. This flexible PVA/PANI/WS<sub>2</sub> film provided a potential application in flexible supercapacitor.

---

**Keywords:** Flexible films, WS<sub>2</sub> nanosheets, Polyaniline, Supercapacitors

### 1. INTRODUCTION

With the serious depletion of non-renewable energy, environmentally friendly energy storage devices have attracted more and more interest [1, 2]. Supercapacitor is a novel energy storage device which is between traditional capacitors and secondary batteries owing to its fast charge-discharge rate, high power density, promising cycle stability, variable working temperature range and environmental protection [3-5]. Currently, supercapacitor contains electrochemical double-layer capacitor (EDLCs) and pseudocapacitors. EDLCs mainly use the carbon materials as electrode materials [6]. The specific capacitance of carbon materials is relatively low. However, pseudocapacitor has high specific capacitance because it uses metal oxides [7], transition metal dichalcogenides [8] and conducting polymers (CPs) [9-11] as electrode materials, which have high electrochemical behaviors.

WS<sub>2</sub> nanosheet has absorbed much notice as the electroactive material due to the W atom has a range of oxidation states from +2 to +6 [12]. However, in fact, it suffers from the low capacitance performance. The mainly explanation is that the nanosheets are restacked leading to the lower conductivity as well as the relative brittle of WS<sub>2</sub> nanosheets [13]. In order to improve the capacitance performance, many composites based on WS<sub>2</sub> have been prepared, such as WS<sub>2</sub>/PEDOT: PSS [14], WS<sub>2</sub>/RGO [15], WS<sub>2</sub>/SWCNT [16], Fe<sub>3</sub>O<sub>4</sub>/WS<sub>2</sub> [17], PEDOT/WS<sub>2</sub> [18] and ZnWO<sub>4</sub>@WS<sub>2</sub> [19]. Polyaniline (PANI) has been considered as a potential candidate for storage devices due to PANI has the highest theoretical specific capacitance among CPs [20]. Currently, there are few reports on the composite of PANI and WS<sub>2</sub> for supercapacitors [21, 22].

Here, a flexible PVA/PANI/WS<sub>2</sub> composite film was firstly prepared through the freezing/thawing method of PVA/aniline/WS<sub>2</sub> hydrogel and following electrochemical deposition. As-prepared PVA/PANI/WS<sub>2</sub> film was characterized by different technologies. The capacitance performance of PVA/PANI/WS<sub>2</sub> composite was performed by cyclic voltammetry (CV), galvanostatic charge-discharge (GCD) and electrochemical impedance spectroscopy (EIS). It was found that the flexible PVA/PANI/WS<sub>2</sub> composite film had good capacitance performance.

## 2. EXPERIMENTAL

### 2.1 Materials

WS<sub>2</sub> (99.9%) power was from Energy Chemical Co., Ltd. N-butyllithium was obtained from Energy Chemical Co., Ltd. N-hexane and aniline (bidistilled before use) are bought from J&K Chemical Reagent Co., Ltd. Polyvinyl alcohol (PVA) was bought from Aladdin Reagent Co., Ltd, (Tianjin, China). Phosphoric acid (H<sub>3</sub>PO<sub>4</sub>) was purchased from Aladdin Reagent Co., Ltd. Doubly distilled water was used throughout the work.

### 2.2 Preparation of PVA/PANI/WS<sub>2</sub> film

WS<sub>2</sub> nanosheets were fabricated using lithium intercalation-exfoliation method [14]. For the fabrication of PVA/PANI/WS<sub>2</sub> film, 0.2 g PVA and 0.2 mL H<sub>3</sub>PO<sub>4</sub> were added in 10 mL deionized water. After that, this solution was heated at 90 °C with mechanical agitation and changed into a transparent solution. And then, 0.2 g anilines were put into the transparent solution and stirred for 10 min. Subsequently, 1.0 mg WS<sub>2</sub> nanosheets were added to the above PVA/aniline solution and stirred for 10 min. The PVA/aniline/ WS<sub>2</sub> solution was cooled at -76 °C and formed the PVA/aniline/WS<sub>2</sub> hydrogel. Finally, the PVA/PANI/WS<sub>2</sub> film was prepared by the CV polymerization of PVA/aniline/WS<sub>2</sub> hydrogel in 1.0 M H<sub>2</sub>SO<sub>4</sub> solution.

### 2.3 Characterizations

The morphology was characterized by scanning electron microscopy (SEM, ZEISS SUPRA 40, German). X-ray photoelectron spectroscopy (XPS, Escalab 250Xi, Al Ka, Thermo Fisher Scientific) was used to investigate the elemental composition of the film. The elementary composition was determined by energy dispersive X-ray spectrometry (EDS, X-Max, Oxford). All the electrochemical characterizations were obtained with an electrochemical workstation (CHI660E, Shanghai Chenhua Instrumental Co., Ltd., China). The electrochemical properties of PVA/PANI/WS<sub>2</sub> composite film as working electrode was tested in 1.0 M H<sub>2</sub>SO<sub>4</sub> solution. The counter electrode and the reference electrode are platinum foil and saturated calomel electrode (SCE), respectively. The specific capacitance was calculated from following Equations [11].

$$C_1 = \frac{\int_{E_1}^{E_2} i(E)d(E)}{2vS_1(E_2-E_1)} \quad (1)$$

$$C_2 = \frac{I \times \Delta t}{S_1 \Delta V} \quad (2)$$

Where  $C_1$ ,  $C_2$  are the areal capacitance,  $\int_{E_1}^{E_2} i(E)d(E)$  is the integrated area of the CV curve,  $i(E)$  is the current density,  $v$  is the scan rate,  $E_1$  and  $E_2$  are the cut off potentials in cyclic voltammetry, and  $S_1$  is the area of the electrode material,  $I$  is the discharge current,  $\Delta t$  is the discharge time,  $S_1$  is the area of the electrode material,  $\Delta V$  was the potential window.

### 3. RESULTS AND DISCUSSION

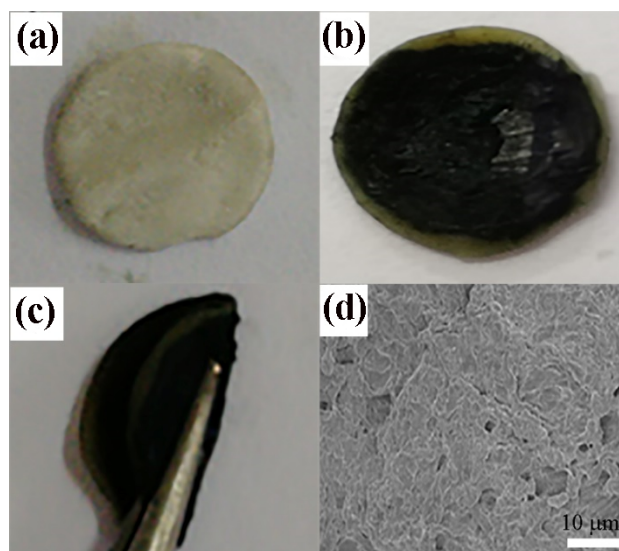


**Figure 1.** Digital photograph of PVA/aniline/WS<sub>2</sub> hydrogel (a) and PVA/PANI/WS<sub>2</sub> film (b, c) and SEM image (d) of PVA/PANI/WS<sub>2</sub> film.

As shown in Fig. 1a, PVA/aniline/WS<sub>2</sub> hydrogel showed a faint yellow film due to the presence of a small amount of WS<sub>2</sub> nanosheets. After the electrochemical reaction of PVA/aniline/WS<sub>2</sub> hydrogel in 1.0 M H<sub>2</sub>SO<sub>4</sub> solution, the color of film was changed into black from faint yellow (Fig. 1b), which

indicated that aniline in hydrogel film has been electropolymerized into PANI. As-prepared PVA/PANI/WS<sub>2</sub> film showed good flexibility (Fig. 1c). From SEM, the PVA/PANI/WS<sub>2</sub> film had a compact surface.

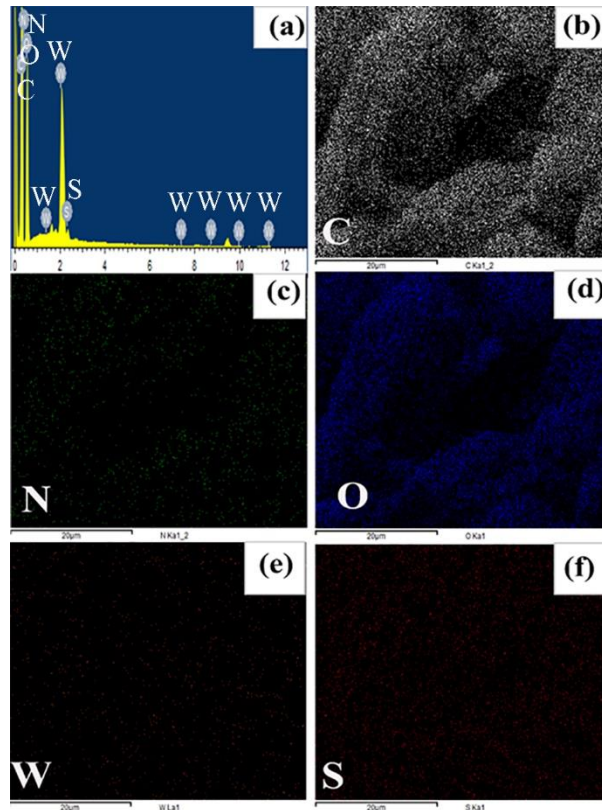


**Figure 2.** EDS (a) of PVA/PANI/WS<sub>2</sub> and EDS mappings of C (b), N (c), O (d), W (e) and S (f) elements in film.

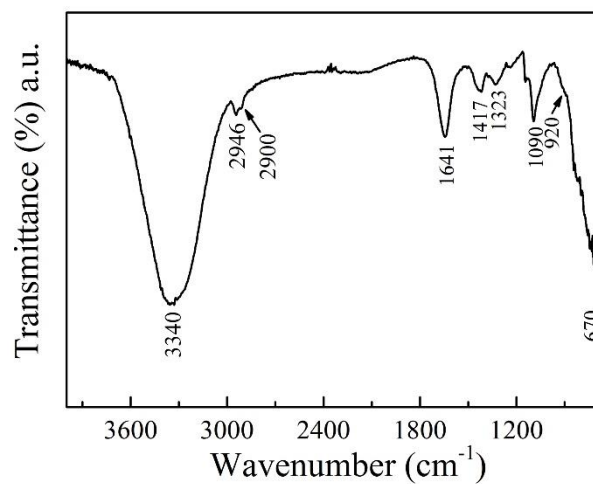


**Figure 3.** FT-IR of PVA/PANI/WS<sub>2</sub> film.

The elemental composite of the as-prepared PVA/PANI/WS<sub>2</sub> film has been tested by EDS (Fig. 2). It was seen from Fig. 2a that the C, N, O, W and S elements were measured, which demonstrated the formation of PVA/PANI/WS<sub>2</sub> composite. The element mappings (Fig. 2b-f) display the uniform dispersion of C, N, O, W and S in the PVA/PANI/WS<sub>2</sub> film.

In the FT-IR of PVA/PANI/WS<sub>2</sub> film (Fig. 3), these peaks located at 1641, 1417 and 1323 cm<sup>-1</sup> were illustrated the stretching vibrations of C=C, C-C and -C-N of PANI. The peaks at 2946, 2900, and 1090 cm<sup>-1</sup> were ascribed to the vibrations of C-H and C-O bonds of PVA, respectively. The broadband present at 3340 cm<sup>-1</sup> was attributable to the -OH and -NH<sub>2</sub> stretching vibrations of PVA and PANI. The peaks at 920 and 670 cm<sup>-1</sup> were assigned to the vibrations of S-S and W-S [23], respectively. These data indicated the presence of PANI, PVA, and WS<sub>2</sub> in the film.

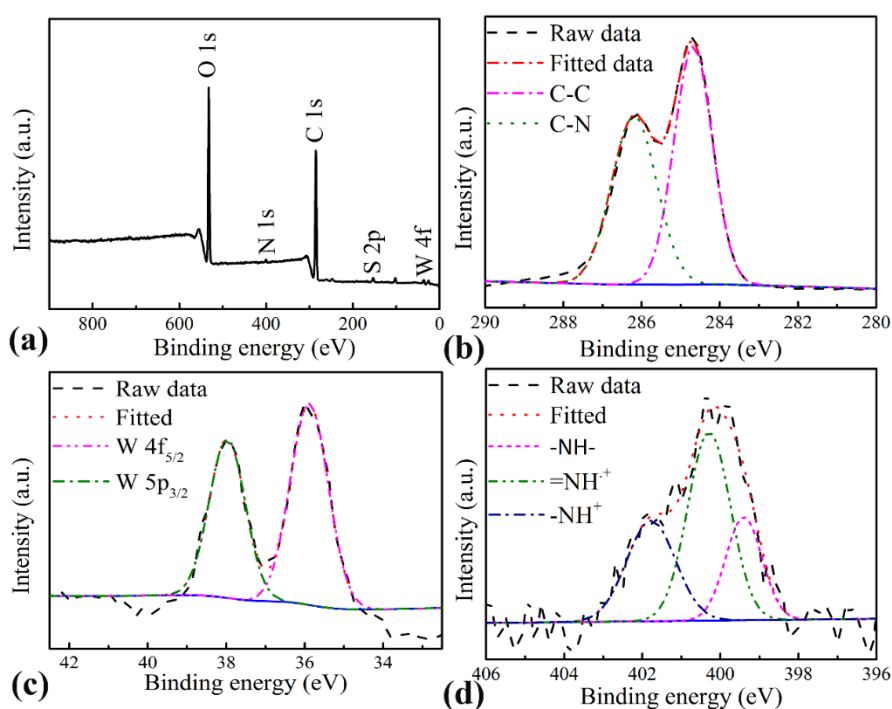


**Figure 4.** XPS pattern of PVA/PANI/WS<sub>2</sub> composite film, (a) The XPS survey spectra of the composite, (b) C, (c) W and (d) N.

To further prove the surface composition of the PVA/PANI/WS<sub>2</sub> composite film, the XPS was carried out. As shown in Fig. 4a, the XPS survey spectrum of the composite was consist of C, N, O, S, and W, which indicated that the PVA/PANI/WS<sub>2</sub> composite film was successfully fabricated. From the Fig. 4b, the core-level spectrum of C 1s was deconvoluted into two peaks at 284.8 eV and 285.4 eV, which were attributed to the bending C-C and C-N, respectively. Fig. 4c demonstrates the peaks located at 35.5 eV and 37 eV, attributing to W 4f<sub>5/2</sub> and W 5p<sub>3/2</sub>, which are characteristic of the W<sup>4+</sup> and W<sup>6+</sup>, respectively [24-26]. Fig. 4d displays three peaks centered at 400.3 eV, 399.5 eV and 401.7 eV, which are attributed to -NH-, =NH<sup>+</sup> and -NH<sup>+</sup>, respectively [27]. Therefore, the results of EDS and XPS fully proved that composite film included PVA, PANI, and WS<sub>2</sub>.

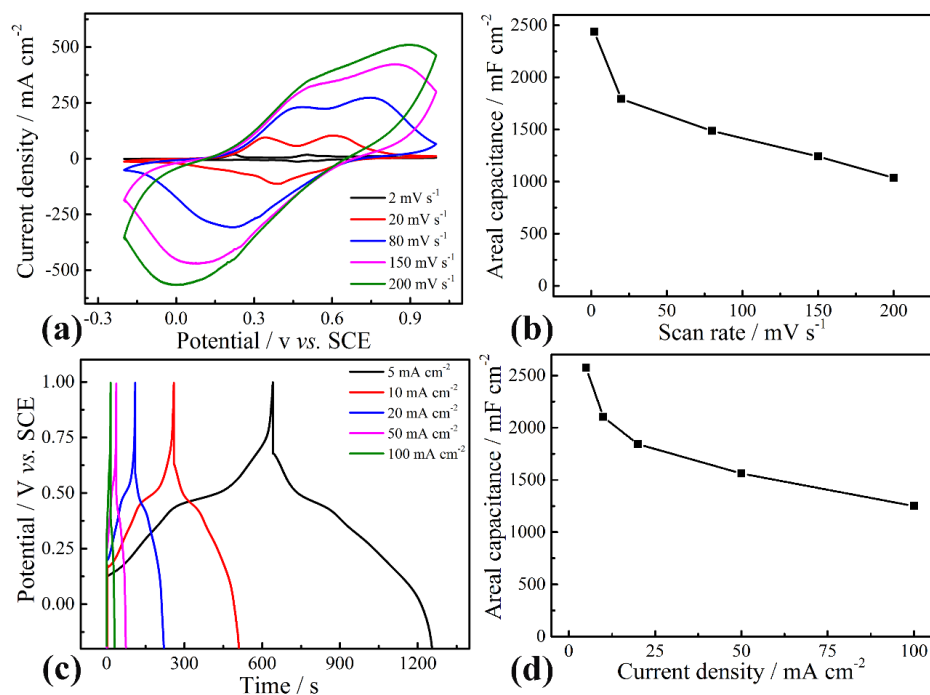


**Figure 5.** (a) CV of PVA/PANI/WS<sub>2</sub> composite film. (b) Specific capacitances as a function of the scan rates. (c) GCD of PVA/PANI/WS<sub>2</sub> film. (d) Specific capacitances as a function of the current densities.

**Table 1.** Comparison of capacity performance of PVA/PANI/WS<sub>2</sub> composite film with other materials.

Electrode material	Electrolyte	Current density/Scan rate	Specific capacitance	Ref.
MoS <sub>2</sub> -pCMF	2 M KCl	5 mV s <sup>-1</sup>	125 mF cm <sup>-2</sup>	[28]
WS <sub>2</sub> /PEDOT:PSS film	1.0 M H <sub>2</sub> SO <sub>4</sub>	40 mV s <sup>-1</sup>	86 mF cm <sup>-2</sup>	[14]
PEDOT/MoS <sub>2</sub> nanocomposite	1.0 M KCl	1.0 mA cm <sup>-2</sup>	149.8 mF cm <sup>-2</sup>	[29]
WO <sub>3</sub> @WS <sub>2</sub>	0.1 M Na <sub>2</sub> SO <sub>4</sub>	5 mV s <sup>-1</sup>	47.5 mF cm <sup>-2</sup>	[13]
WS <sub>2</sub> /carbon cloth	5 M LiCl	4 mA cm <sup>-2</sup>	930 mF cm <sup>-2</sup>	[30]
Graphite/PANI	1.0 M H <sub>2</sub> SO <sub>4</sub>	0.5 mA cm <sup>-2</sup>	355.6 mF cm <sup>-2</sup>	[31]
PANI/PVA hydrogel	1.0 M H <sub>2</sub> SO <sub>4</sub>	1 A g <sup>-1</sup>	2320 mF cm <sup>-2</sup>	[32]
CNT/PANI hydrogel	1.0 M H <sub>2</sub> SO <sub>4</sub>	1 mA cm <sup>-2</sup>	680 mF cm <sup>-2</sup>	[33]
V <sub>2</sub> O <sub>5</sub> /PANI	5 M LiCl	0.5 mA cm <sup>-2</sup>	664.5 mF cm <sup>-2</sup>	[34]
PVA/PANI/WS <sub>2</sub> film	1.0 M H <sub>2</sub> SO <sub>4</sub>	2 mV s <sup>-1</sup> 200 mV s <sup>-1</sup>	2437 mF cm <sup>-2</sup> 1048 mF cm <sup>-2</sup>	This work

The electrochemical properties of PVA/PANI/WS<sub>2</sub> composite film (effective area:  $S_1 = 0.28 \text{ cm}^2$ ) were investigated by CV, GCD, and EIS. Fig. 5a shows the CV curves of PVA/PANI/WS<sub>2</sub> composite film, the redox peaks in CVs were attributed to the oxidation and reduction reaction of WS<sub>2</sub> and PANI.

The specific capacitance of PVA/PANI/WS<sub>2</sub> composite film reached 2437 mF cm<sup>-2</sup> at 2 mV s<sup>-1</sup>, with the scan rate of increasing to 200 mV s<sup>-1</sup>, the specific capacitance still maintained at 1048 mF cm<sup>-2</sup> (Fig. 5b). Moreover, in Fig. 5c, the GCD showed a nearly symmetrical curves with large IR drop. The large IR drop mainly came from the large ions diffusion resistance. With increasing the current density from 5 mA cm<sup>-2</sup> to 100 mA cm<sup>-2</sup>, the specific capacitance decreased from 2572.5 mF cm<sup>-2</sup> to 1250.7 mF cm<sup>-2</sup>. The specific capacitance of PVA/PANI/WS<sub>2</sub> composite film was higher than those of other electrode materials (Table 1). This indicated that the flexible PVA/PANI/WS<sub>2</sub> composite film would be a potential electrode material for supercapacitors.

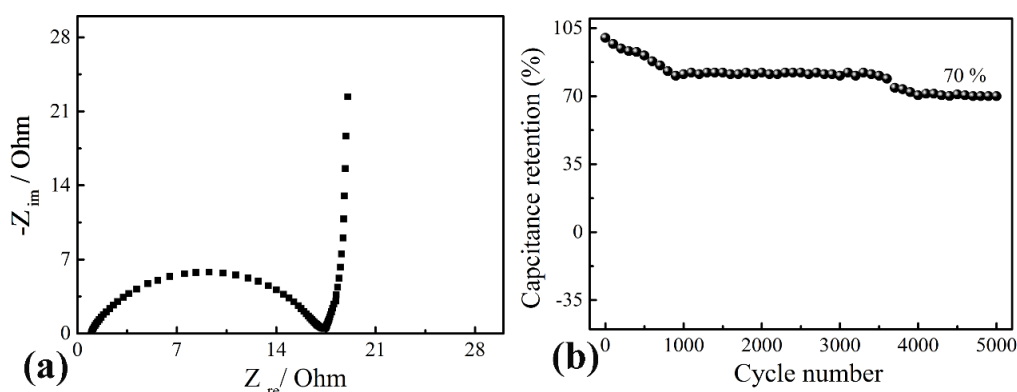


**Figure 6.** Nyquist plots (a) and long-term cycle stability (b) of PVA/PANI/WS<sub>2</sub> composite film.

To further evaluate the electrochemical behaviors of the PVA/PANI/WS<sub>2</sub> composite film, EIS was measured over a range of 0.01 Hz to 10<sup>5</sup> Hz. Fig. 6a shows the Nyquist of the PVA/PANI/WS<sub>2</sub> composite film. At high-frequency region, a semicircle was observed, and the diameter of semicircle defined as the charge transfer resistance of electrode ( $R_{ct}$ ), the  $R_{ct}$  value of the PVA/PANI/WS<sub>2</sub> composite film was 16.5 ohm. The line at the low-frequency region was slightly deviated from the vertical line. This was due to the pseudocapacitance behaviors of PANI and WS<sub>2</sub> [35]. It is well-known that the cycle stability plays a significant role on the electrode material. Fig. 6b shows the cycle stability of PVA/PANI/WS<sub>2</sub> composite film at 100 mA cm<sup>-2</sup>. At the first 500 cycles, the specific capacitance decreased to 90% of initial specific capacitance. After 5000 cycles, the PVA/PANI/WS<sub>2</sub> film had 70% retention of the initial specific capacitance. The capacitance retention was higher than that of PANI. For example, PANI nanowire had 40% capacitance retention after 5000 cycles [36]; PANI film showed 36% capacitance retention after 50 cycles [37].

#### 4. CONCLUSIONS

In summary, a flexible PVA/PANI/WS<sub>2</sub> composite film was successfully prepared by the electrochemical reaction of the prefabricated PVA/aniline/WS<sub>2</sub> hydrogel. The specific capacitance of the PVA/PANI/WS<sub>2</sub> composite film reached 2437 mF cm<sup>-2</sup> at 2 mV s<sup>-1</sup>. Even at a high scan rate of 200

mV s<sup>-1</sup>, the composite film still had a high specific capacitance of 1048 mF cm<sup>-2</sup>. Moreover, the composite film showed high cycle stability after 5000 cycles. This work provides a new strategy to fabricate flexible PVA/PANI/WS<sub>2</sub> film with high capacitance performance.

#### ACKNOWLEDGEMENTS

This work was supported by the National Natural Science Foundation of China (Grant Nos. 51662012, 51862011, 51762020), Jiangxi Outstanding Young Talent Fund Projects (20171BCB23076).

#### References

1. Y. Z. Zhang, T. Cheng, W. Y. Lai, H. Pang and W. Huang, *Chem. Soc. Rev.*, 44 (2015) 5181.
2. H. Zhou, W. Zhang and X. Zhi, *J. Mater. Sci.-Mater. El.*, 29 (2018) 19078.
3. D. Wang, T. Xue, J. Ma and G. Geng, *J. Power Sources*, 307 (2016) 401.
4. S. Faraji, *J. Power Sources*, 263 (2014) 338.
5. X. Wang, A. Y. Mehandzhyskia, B. Arstadc, K. V Aken, Tyler S. Mathis, A. Gallegosd, Z. Tian, D. Rene, E. Sheridanf, B. A. Grimesa, D. Jiang, J. Wu, Y. Gogotsi and D. Chen, *J. Am. Chem. Soc.*, 139 (2017) 18681.
6. Y. Wang, Y. Song and Y. Xia, *Chem. Soc. Rev.*, 45 (2016) 5925.
7. W. Li, X. Wang, N. Zhang and M. Ma, *Angew. Chem.*, 128 (2016) 9342.
8. D. Li, W. Zhou, Q. Zhou, G. Ye, T. Wang, J. Wu, Y. Chang and J. Xu, *Nanotechnology*, 28 (2017) 395401.
9. L. Dong, Y. Li, Z. H. Huang, F. Kang, Q. H. Yang and X. Zhao, *J. Mater. Chem. A*, 4 (2016) 4659.
10. D. Mo, W. Zhou, X. Ma and J. Xu, *Electrochim. Acta*, 155 (2015) 29.
11. Q. Zhou, D. Zhu, X. Ma, J. Xu, W. Zhou and F. Zhao, *RSC Adv.*, 6 (2016) 29840.
12. C. C. Tu, B. C. Xiao and Y. S. Chen, *J. Power Sources*, 320 (2016) 78.
13. N. Choudhary, H. S. Chung, J. Moore, J. Thomas and Y. Jung, *ACS Nano*, 10 (2016) 10726.
14. A. Liang, D. Li, W. Zhou, Y. Wu, G. Ye, J. Wu, Y. Chang, R. Wang, J. Xu, G. Nie, J. Hou and Y. Du, *J. Electroanal. Chem.*, 824 (2018) 136.
15. S. Ratha and C. S. Rout, *ACS Appl. Mater. Inter.*, 5 (2013) 11427.
16. J. Ren, Z. Wang, F. Yang, R. P. Ren and Y. K. Lv, *Electrochim. Acta*, 267 (2018) 133.
17. Y. Dai, M. Chen, X. Yan, J. Wang, Q. Wang, C. Zhou, D. Wang, H. Zhang, Y. Wang and X. Cheng, *J. Nanosci. Nanotechno.*, 19 (2019) 897.
18. X. Xiao, C. Engelbrekt, M. Zhang, Z. Li, J. Ulstrup, J. Zhang and P. Si, *Appl. Surf. Sci.*, 410 (2017) 308.
19. T. Anitha, A. E. Reddy, I. K. Durga, S. S. Rao, H. W. Nam and H. J. Kim, *J. Electroanal. Chem.*, 841 (2019) 86.
20. K. Lota, V. Khomenko and E. Frackowiak, *J. Phys. Chem. Solids*, 65 (2004) 295.
21. K. Gopalakrishnan, S. Sultan, A. Govindaraj and C. N. R. Rao, *Nano Energy*, 12 (2015) 52.
22. M. Martinez, J. G. S. Moo, B. Khezri, P. Song, A. C. Fisher, Z. Sofer and M. Pumera, *Adv. Funct. Mater.*, 26 (2016) 6662.
23. A. Khataee, P. Eghbali, M. H. I. Nezhad and A. Hassani, *Ultrason. Sonochem.*, 48 (2018) 329.
24. S. X. Leong, C. C. M. Martinez, X. Chia, J. Luxa, Z. Sofer and M. Pumera, *ACS Appl. Mater. Inter.*, 9 (2017) 26350.
25. K. Tang, X. Wang, Q. Li and C. Yan, *Adv. Mater.*, 30 (2018) 1704779.
26. X. Wang, X. Gan, T. Hu, K. Fujisawa, Y. Lei, Z. Lin, B. Xu, Z. H. Huang, F. Kang, M. Terrones and R. Lv, *Adv. Mater.*, 29 (2017) 1603617.
27. Y. Luo, D. Kong, Y. Jia, J. Luo, Y. Lu, D. Zhang, K. Qiu, C. M. Li and T. Yu, *RSC Adv.*, 3 (2013) 5851.

28. N. Islam, S. Wang, J. Warzywoda and Z. Fan, *J. Power Sources*, 400 (2018) 277.
29. D. Li, D. Zhu, W. Zhou, Q. Zhou, T. Wang, G. Ye, L. Lv and J. Xu, *J. Electroanal. Chem.*, 801 (2017) 345.
30. S. Liu, Y. Zeng, M. Zhang, S. Xie, Y. Tong, F. Cheng and X. Lu, *J. Mater. Chem. A*, 5 (2017) 21460.
31. B. Yao, L. Yuan, X. Xiao, J. Zhang, Y. Qi, J. Zhou, J. Zhou, B. Hu and W. Chen, *Nano Energy*, 2 (2013) 1071.
32. W. Li, X. Wang, N. Zhang and M. Ma, *Angew. Chem. Int. Ed.*, 55 (2016) 9196.
33. S. Zeng, F. Cai, Y. Kang, M. Chen and Q. Li, *J. Mater. Chem., A*, 3 (2015) 23864.
34. M. H. Bai, T. Y. Liu, F. Luan, Y. Li and X. X. Liu, *J. Mater. Chem. A*, 2 (2014) 10882.
35. Y. Zhang, W. Sun, X. Rui, B. Li, H. T. Tan, G. Guo, S. Madhavi, Y. Zong and Q. Yan, *Small*, 11 (2015) 3694.
36. T. Liu, L. Finn, M. Yu, H. Wang, T. Zhai, X. Lu, Y. Tong and Y. Li, *Nano Lett.*, 14 (2014) 2522.
37. W. Qin, L. J. ling, G. Fei, L. W. Sheng, W. K. Zhong and W. X. Dong, *New Carbon Mater.*, 23 (2008) 275.

© 2020 The Authors. Published by ESG ([www.electrochemsci.org](http://www.electrochemsci.org)). This article is an open access article distributed under the terms and conditions of the Creative Commons Attribution license (<http://creativecommons.org/licenses/by/4.0/>).